

Design Feature

TIAN-PENG LI | Engineer GUANG-MING WANG | Engineer CHEN-XIN ZHANG | Engineer BIN-FENG ZONG | Engineer

Air and Missile Defense College, Air Force Engineering University, Xi'an, Shaanxi 710051, People's Republic of China,
e-mail: ltp19880812@163.com

Novel Transmission Line Impacts Antenna Design

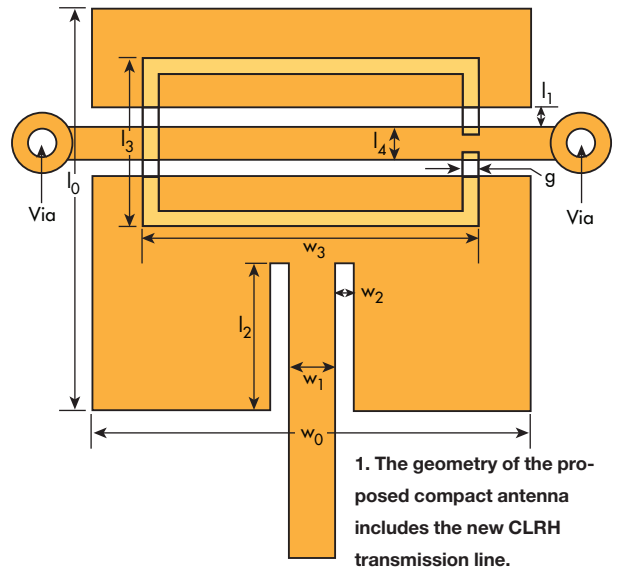
This antenna design approach takes advantage of composite-right/left-handed (CRLH) transmission lines to shrink the size of patch antennas.

Demand for electrically small antennas continues to soar, particularly among mobile electronic applications. Though the benefits are significant, these antennas aren't the easiest to achieve. Use of a novel composite-right/left-handed (CRLH) transmission line, however, facilitates the creation of these antennas. A CRLH transmission line incorporates a ground plane with an etched complementary single split-ring resonator (CSSRR) and a patch with two series gaps and two metal viaholes.

Based on a CRLH transmission-line unit cell, an antenna was designed and fabricated, and found to provide a -10 -dB impedance bandwidth of 5.63% at 3 GHz. The compact antenna patch measures only $0.2\lambda_0 \times 0.17\lambda_0 \times 0.01\lambda_0$ —a 69.1% reduction in size compared to a conventional patch antenna. The compact antenna design ultimately achieved peak gain of 4.29 dB.

Some of these electrically small antennas exploit the electromagnetic (EM) characteristics of CRLH transmission lines. Since the realization of resonant frequency of a zeroth-order resonator (ZOR) is independent of its dimensions, but is determined by the configuration of the unit cells, there's been a spate of ZOR-based miniaturized antennas proposed of late.¹ Unfortunately, these devices are often limited in terms of bandwidth.

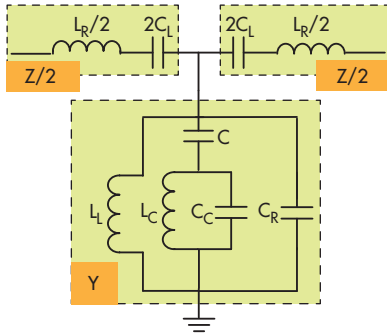
By combining a TM₁₀ transmission mode and a ZOR mode, however, some antennas increased half-power beamwidth by 53% over conventional rectangular patch antennas, with a boost in antenna bandwidth of 3.3%.² In one study,³ a hybrid mode was proposed in which a wideband patch antenna with TM₀₁ and TM₁₀ modes was loaded with a planar CRLH unit cell to enhance its bandwidth. However, its size only shrank by 45% when compared to a conventional rectangular patch antenna.



CRLH TRANSMISSION-LINE INNOVATION

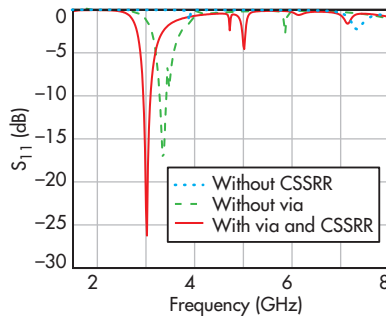
To maintain antenna performance with reduced size, a new type of CRLH transmission-line structure was developed. It reduces the resonant frequency by loading with a complementary single split-ring resonator (CSSRR) for shunt inductance and a patch slot for series capacitance. Furthermore, two symmetric viaholes were incorporated to change the shunt inductance. These techniques made it possible to implement a CRLH unit cell in fully planar technology, toward the design of a compact antenna.

Figure 1 shows the geometry of the proposed antenna's geometry. A patch with two series gaps and two short stubs forms on the top side, and a CSSRR slot is etched on the ground plane on the bottom side. The two white circles denote metallic viaholes.



2. This is an equivalent-circuit model of the proposed antenna.

According to CRLH transmission-line theory, the equivalent-circuit model of the proposed antenna can be depicted as that in Fig. 2. Since the patch provides series inductance and the gaps yield series capacitance, the patch with two series gaps is represented as a series LC circuit (L_R and C_L), while the CSSRR slot is represented as a shunt LC resonant tank (C_C and L_C).⁴ On the other hand, the capacitance between the patch and the ground plane capacitance (C) connects the shunt resonant tank to the patch, while capacitance C_R connects the ground with the patch. The two metallic viasoles connected with two short stubs are described by shunt inductance L_L , connecting the patch with ground.



3. S_{11} responses are compared for three types of antennas.

$$\beta_d = \cos^{-1} \left(1 + \frac{(1 - \frac{\omega^2}{\omega_{se}^2})(\frac{C}{C_L} - \frac{\omega^2}{\omega_C^2})}{2(1 - \frac{\omega^2}{\omega_Z^2})} - \frac{(1 - \frac{\omega^2}{\omega_{se}^2})(1 - \frac{\omega^2}{\omega_{sh}^2})}{2\frac{\omega^2}{\omega_L^2}} \right)$$

and

$$\omega_{se} = \frac{1}{\sqrt{L_R C_L}} \quad \omega_{sh} = \frac{1}{\sqrt{L_L C_R}} \quad (2)$$

$$\omega_R = \frac{1}{\sqrt{L_R C_R}} \quad \omega_L = \frac{1}{\sqrt{L_L C_L}}$$

$$\omega_C = \frac{1}{\sqrt{L_C C_C}} \quad \omega_Z = \frac{1}{\sqrt{L_C (C_C + C)}}$$

EXODUS

ADVANCED COMMUNICATIONS

High Power Amplifiers / Low Noise Amplifiers / Waveguide Components / Antennas & Cavity Filters
Modules & Systems / Power Levels available up to 3KW / Frequencies available up to 37GHz

EXODUS ADVANCED COMMUNICATIONS

Exodus Advanced Communications, Corp.
170 S. Green Valley Parkway Suite 300 Henderson, NV 89012 U.S.A.
Tel : 1-702-534-6564 Fax : 1-702-441-7016
Email : sales@exoduscomm.com Web : www.exoduscomm.com

Sales contacts
Inside Sales : Christy Strahan Anderson
Domestic/International Sales : Bill Liebman
Technical Sales : Effi Bainvoll

Based on the analysis above, one can safely conclude that a model circuit is provided by a complex CRLH transmission-line circuit: C_L represents the left-handed capacitance; L_C and L_L represent the left-handed inductance; C and C_C represent the right-handed capacitance; and L is the right-handed inductance. From the equivalent-circuit model, the dispersion relation can be expressed as Eq. 1:

$$\beta_d = \cos^{-1}(1 + ZY/2) \quad (1)$$

where β_d = the length of the unit cell,

and

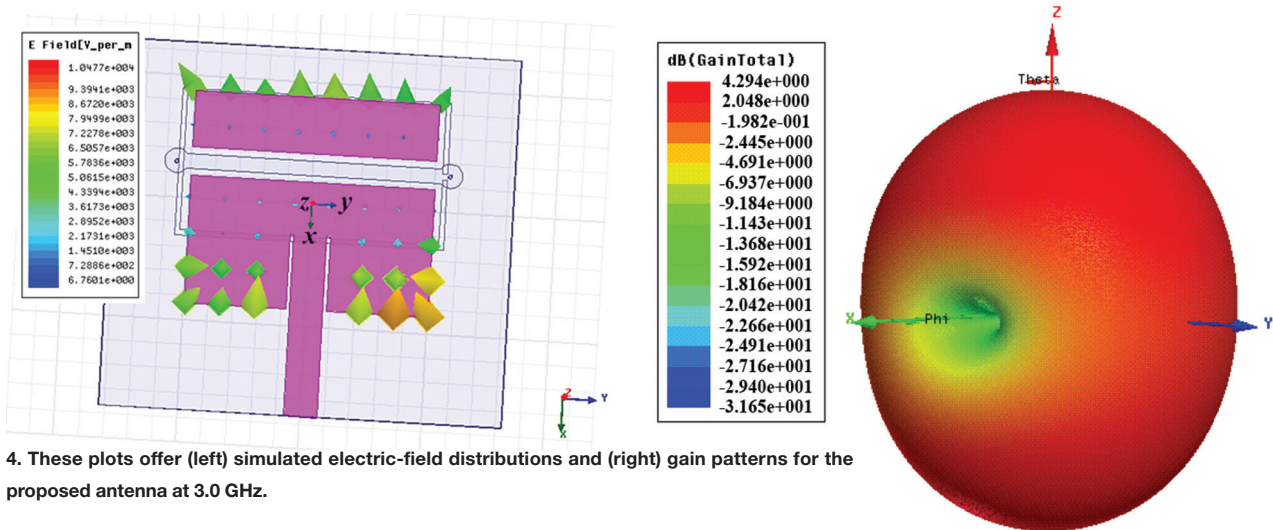
$$Z = j\omega L_R + 1/(j\omega C_L)$$

and

$$Y = [j\omega C/(j\omega C_C + 1/j\omega L_C + 1/j\omega L_L)] + j\omega C_R$$

represent the series impedance and shunt admittance, respectively. The dispersion relation can be determined by means of Eq. 2 (see above).

Visit us at IMS Show Booth # 3014



4. These plots offer (left) simulated electric-field distributions and (right) gain patterns for the proposed antenna at 3.0 GHz.

In another way, it's possible to obtain the resonant modes of the CRLH transmission line by applying Eq. 3:

$$\beta_d = n\pi \quad (n = -1, 0, +1) \quad (3)$$

With these relationships, the negative first-order resonance, the ZOR, and the positive first-order resonance can be obtained according to Eqs. 5 and 6. At the ZOR, the phase constant (β_d) becomes zero and infinite wavelength propagation is theoretically possible, although the working bandwidth is narrow.

The negative first-order resonance supports backward-wave propagation with the same field distribution as the positive first-order resonance. Nonetheless, the resonance generally has such low efficiency that it cannot be used for antenna radiation purposes.⁵

ANTENNA ANALYSIS

Analyzing the antenna design can be somewhat complicated. Considering the shunt part, there are four relevant resonant frequencies relative to the shunt impedance based on this circuit model: two frequencies that null the corresponding admittance (ω_C and ω_L), a shunt resonant frequency (ω_{sh}), and a transmission-zero frequency (ω_Z). Parameters ω_C , ω_{sh} , ω_Z were previously explained in Eq. 3, and the relationship for ω_L is given in Eq. 4:^{6,7}


$$\omega_L = \frac{1}{\sqrt{L_C \left(C_C + \frac{4}{\frac{1}{C_L} + \frac{1}{C}} \right)}} \quad (4)$$

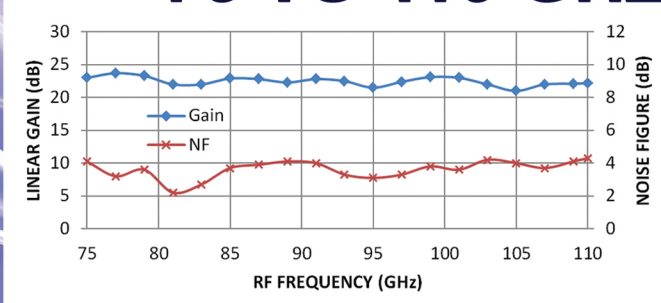
The resonant efficiency is low at ω_{sh} and the right-handed

**IMS2015
BOOTH
#2009**


LOW NOISE AMPLIFIER 75 TO 110 GHz


**4 dB
NOISE FIGURE**





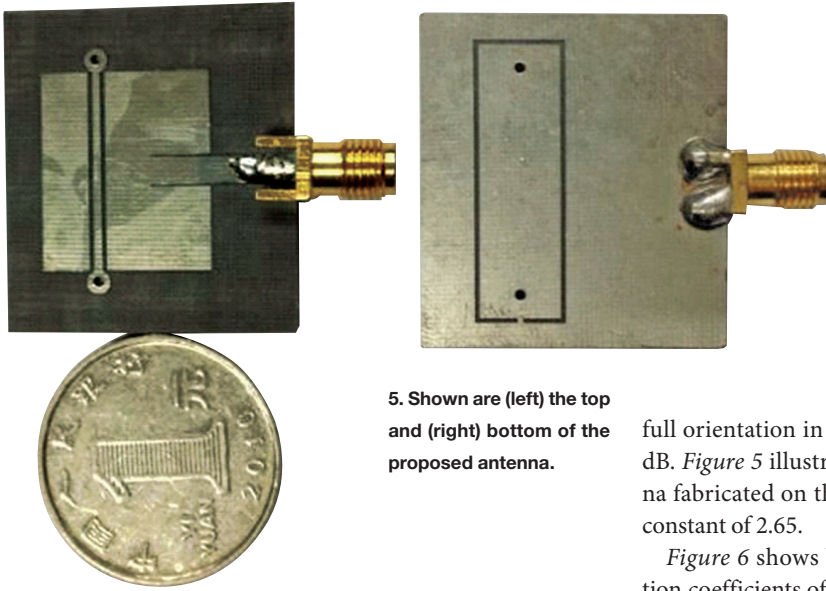
RF Frequency (GHz)	Linear Gain (dB)	Noise Figure (dB)
75	23	4
80	23	4
85	23	4
90	23	4
95	23	4
100	23	4
105	23	4
110	23	4





MADE IN USA

www.sagemillimeter.com | 3043 Kashiwa Street, Torrance, CA 90505
T: 424-757-0168 | F: 424-757-0188 | sales@sagemillimeter.com



5. Shown are (left) the top and (right) bottom of the proposed antenna.

resonant efficiency (ω_R) often measures higher than is the case in practice applications.

Simulations of an antenna model were performed for a Teflon circuit substrate material with relative dielectric constant (ϵ_r) of 2.65, $\tan \delta$ of 0.001, and thickness of 1 mm. The simulations were performed using the High-Frequency Structure Simulator (HFSS) software from Keysight Technologies (www.keysight.com), based on the finite-element method with the following dimensions: $w_0 = 20$ mm; $w_1 = 2.72$ mm; $l_0 = 17.4$ mm; $l_1 = 0.5$ mm; and $g = 0.6$ mm. Because the dimensions w_3 and l_3 are related to the shunt resonance, modifications to those dimensions result in changes to the resonant frequency, while modifications to dimensions w_2 and l_2 lead to impedance matching.

Figure 3 compares reflection coefficients (S_{11}) for the proposed antenna without CSSRR, without viaholes, and with CSSRR and viaholes. The antenna with viaholes and CSSRR achieves a multiple-resonant frequency response with reduced frequency compared to the other two approaches.

For the best radiated performance, the antenna dimensional parameters were optimized for the following values: $w_0 = 20$

mm; $w_1 = 2.72$ mm; $l_0 = 17.4$ mm; $l_1 = 0.5$ mm; $g = 0.8$ mm; $w_2 = 0.3$ mm; $l_2 = 6.1$ mm; $w_3 = 22$ mm; $l_3 = 14$ mm; and $l_4 = 0.8$ mm. The radius of the viahole was 0.15 mm.

The simulated electric-field distributions for the proposed compact antenna are depicted in Fig. 4 (left). With the structure's two x-oriented edges being 180 deg. out of phase at 3 GHz, a transverse-magnetic TM₁₀ mode is excited. The simulated gain for the antenna at 3 GHz is given in Fig. 4 (right), with

full orientation in the Y_0Z plane and maximum gain at 4.29 dB. Figure 5 illustrates the prototype of the proposed antenna fabricated on the Teflon substrate with relative dielectric constant of 2.65.

Figure 6 shows both the simulated and measured reflection coefficients of the proposed antenna. The measured data were in good agreement with the simulated results, with just a few exceptions. The measured 10-dB return-loss bandwidth equaled 170 MHz (5.6%) from 2.94 to 3.11 GHz. The electrical size of the radiating patch featured dimensions of $0.2\lambda_0 \times 0.17\lambda_0 \times 0.01\lambda_0$ ($20 \times 17.4 \times 1$ mm) at a center frequency of 3.02 GHz.

Owing to the CRLH structure and use of metal viaholes to enhance the shunt inductance, antenna size was reduced 69.1%, compared to a conventional patch antenna measuring $37 \times 30.4 \times 1$ mm. Even with this dramatic size reduction, the microstrip patch antenna provides strong performance at its 3.02-GHz center frequency. **tmw**

ACKNOWLEDGMENT

This work is supported by the National Natural Science Foundation of China under Grant No. 61372034.

REFERENCES

1. T. Ueda, G. Haida, and T. Itoh, "Zeroth-order resonators with variable reactance loads at both ends," IEEE Transactions on Microwave Theory & Techniques, Vol. 59, No. 3, 2011, pp. 612-618.
2. S.T. Ko and J.-H. Lee, "Hybrid zeroth-order resonance patch antenna with broad E-plane beamwidth," IEEE Transactions on Antennas & Propagation, Vol. 61, No. 1, 2013, pp. 19-25.
3. J. Ha, K. Kwon, Y.K. Lee, and J. Choi, "Hybrid mode wideband patch antenna loaded with a planar metamaterial unit cell," IEEE Transactions on Antennas & Propagation, Vol. 60, No. 2, 2012, pp. 1143-1147.
4. M. Gil, J. Bonache, J. G. Garcia, J. Martel, and F. Martin, "Composite right/left-handed metamaterial transmission lines based on complementary split-ring resonators and their applications to very wideband and compact filter design," IEEE Transactions on Microwave Theory & Techniques, Vol. 55, No. 6, 2007, pp. 1296-1304.
5. C. Zhou, G.M. Wang, Y.W. Wang, B.F. Zong, and J. Ma, "CPW-fed dual-band linearly and circularly polarized antenna employing novel composite right/left-handed transmission-line," IEEE Transactions on Antennas & Propagation Letters, Vol. 12, 2013, pp. 1073-1076.
6. Ozgur Isik and Karu P. Esselle, "Backward Wave Microstrip Lines With Complementary Spiral Resonators," IEEE Transactions on Antennas & Propagation, Vol. 56, No. 10, 2008, pp. 3173-3178.
7. M. Gil, J. Bonache, J. Selga, J. Garcia-Garcia, and F. Martin, "Broadband Resonant-Type Metamaterial Transmission Lines," IEEE Microwave and Wireless Component Letters, Vol. 179, No. 2, 2007, pp. 97-99.

6. The plots compare the simulated and measured S_{11} responses for the proposed antenna.

